Use Moving Average Filter to Reduce Noises in Wearable PPG During Continuous Monitoring

Yan Chen, Dan Li(✉), Yanhai Li, Xiaoyuan Ma, and Jianming Wei

Shanghai Advanced Research Institute, Chinese Academy of Sciences,
No.99 Haike Road, Pudong, Shanghai, China
{cheny, lid, liyh, maxy, wjm}@sari.ac.cn

Abstract. In order to improve the accuracy of heart rate extracted from wearable photoplethysmography (PPG) signal, a new processing method based on moving average filtering is proposed. There are two cascaded moving average filters. The first filter is designed to remove baseline wandering as preprocessing. The second filter whose window size is adjusted according to the additional accelerometer signal is used to remove motion artifacts. During continuous monitoring, the parameters of these two filters change adaptively in accordance with a batch processing method. The results show that the proposed method can reconstruct a better waveform and improve the signal quality for calculating the beats per minute (BPM). Referenced with the vital sign monitoring instrument VS800 of Mindray company, the detecting accuracy of the proposed method is 7%–10% higher than adaptive filtering.

Keywords: Heart rate · PPG · Moving average

1 Introduction

With the wide application of wearable devices in the field of health care, the technology of heart rate detection based on PPG is developing rapidly. Wearable PPG technology, consisting of light emitting diode (LED) and photoelectric detector, provide a simple, low cost and noninvasive heart rate detection method [1]. Alternative measurement sites commonly include finger [2], wrist [3] and ear [4]. However, poor reliability and accuracy of heart rate detection bring problems to the practical application. It is mainly because of the motion artifact which is a noise aliasing in the clean PPG signal. In most cases, motion artifacts falls within the same frequency band as the physiological signal of interest [5]. Exercises, especially strenuous exercises (e.g., high leg lifting, quick running, etc.), damage the waveform seriously and affect the measurement of PPG's periodicity, which eventually lead to the error of heart rate.

Sweeny K.T., et al. [6] make a detailed analysis of current artifact removal techniques including adaptive filtering, wiener filtering, bayes filtering and blind source separation. An on-line and automatic processing technique is necessary for wearable devices. Han, H. and Kim J. [7] propose a least mean square based active noise cancellation method applied to accelerometer data to reduce periodical artifacts and

© ICST Institute for Computer Sciences, Social Informatics and Telecommunications Engineering 2017
K. Giokas et al. (Eds.): eHealth 2016, LNICST 181, pp. 193–203, 2017.
DOI: 10.1007/978-3-319-49655-9_26

recover pulse from PPGs efficiently. Gibbs P.T., Wood L.B., and Asada H.H. [8] motivate a recursive least squares active noise cancellation technique using the MEMS accelerometer reading as an input for a FIR or Laguerre model. Lee B., et al. [9] use kalman smoother with simultaneous accelerometry to reduce motion artifacts from PPG signal. These filters calculate and update corresponding coefficients by sampling point. There is high time complexity in these algorithms and most of them are not able to remove burst noises during continuous monitoring perfectly.

We consider the ear is the best measurement site as there is no movable joints. We integrate LED, photoelectric sensor and accelerometer sensor into an earphone. In this paper, from the principle of PPG, we propose a simple model of the in-ear PPG signal and analyze different noise sources. Then we design two kind of moving average filters to reduce different noises from the actual PPG signal. This paper also puts forward a batch processing method to adjust the parameters of the filters as the heartbeat and motion state keep changing during continuos monitoring.

2 Analysis

2.1 Principle of PPG

Part of the incident light will be absorbed by vascular tissue, and the transmitted light intensity follows Lambert-Beer's law [10] which is the theoretical basis of understanding PPG:

$$I = I_0 \cdot exp(-\boldsymbol{KCL}) \tag{1}$$

In formula (1), I_0 represents incident light intensity, $\boldsymbol{K}$ is the absorption coefficient which is only related to the physical properties of substances and wavelength of the incident light, $\boldsymbol{C}$ denotes the density, $\boldsymbol{L}$ is the optical path. While our light intensity in-ear photoelectric detector receives is:

$$I = I_1 + \boldsymbol{I}_2 \cdot exp(-\boldsymbol{KCL}) \tag{2}$$

I_1 is the part of light reflected directly. $\boldsymbol{I}_2$ is the light irradiation to skin, muscle and blood vessel. Ideally, the acquired result only changes with the vascular pulsation caused by heart beats, so PPG waveform is an alternating component (AC) superimposed on a direct-current component (DC). Actually, respiratory, nervous sympathetic activity and body temperature changes can cause a slow change of the baseline [11]. The muscle will be squeezed during motion state which will also affect the optical path. The actual light intensity is:

$$\begin{aligned} I &= I_1 + \Delta I + \boldsymbol{I}_2 \cdot exp[-\boldsymbol{KC}(\boldsymbol{L} + \Delta \boldsymbol{L})] \\ &= I_1 + \Delta I + \boldsymbol{I}_2 \cdot exp(-\boldsymbol{KCL}) \cdot [\exp(-\Delta \boldsymbol{L}) - 1 + 1] \end{aligned} \tag{3}$$

Where ΔI represents the change of baseline which is called baseline wandering, $\Delta \boldsymbol{L}$ represents the change of optical path caused by vascular pulsation and muscle squeeze. As $\Delta \boldsymbol{L}$ is extremely little, our PPG signal can be shown as:

$$S = S_0 + \Delta S - S_1 \cdot \Delta L_1 - S_2 \cdot \Delta L_2 \tag{4}$$

Where S_0 is the baseline signal, ΔS is the baseline wandering signal, $S_1 \cdot \Delta L_1$ is the desired signal, and $S_2 \cdot \Delta L_2$ is the motion artifact signal. In order to study the change of motion artifacts signal, we add an accelerometer sensor into the sensing unit.

2.2 Actual PPG Signal

Before proceeding further discussion, it is necessary to check the actual signal waveform. Figure 1 shows a period of actually acquired signal including three axis accelerometer signals and photoelectric signal. The sampling rates are both 62.5 Hz. In order, the motion state is standing, running and standing. From the beginning to the end, the photoelectric signal waveform has a gentle wandering which is called baseline wandering noise. During the running state, the morphology of PPG signal is corrupted seriously as motion artifacts noise exits.

Through Fourier analysis, according to the amplitude spectrum figure, we find that the frequency of motion artifacts is similar to accelerometer signals which is pointed out by Zhang Z.L. [12]. As x axis is the major factor in this case, we only show its amplitude spectrum figure. In Fig. 2, the green arrows pointing at about 2 Hz are motion artifacts, the black arrow nearby 0 Hz represents the baseline wandering and the red arrow neighbouring 1 Hz is the frequency of hear rate we desired. Of course, motion artifacts noise has different forms in different motion states. This rhythmic motion artifact most severely affects the heart rate detection, as it destroys the periodicity and morphology of the PPG signal. In other cases, random irregular motions leading the PPG signal shake suddenly and randomly will also affect the estimated period.

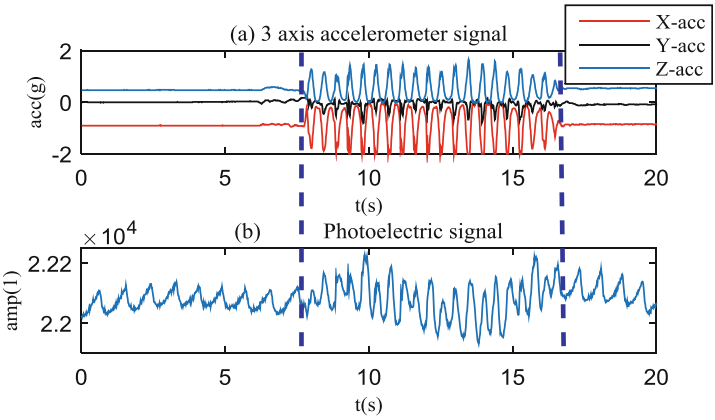

Fig. 1. A period of actual detected signal.

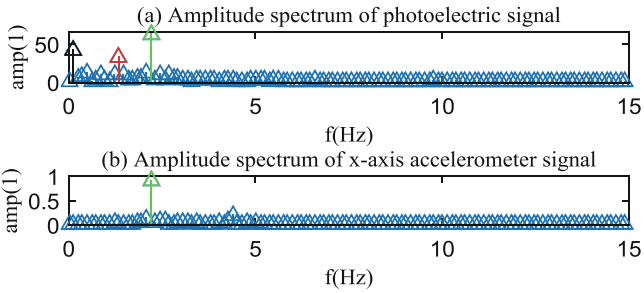

Fig. 2. Fourier analysis of the photoelectric signal and accelerometer signal of Fig. 1 in the running state. (Color figure online)

3 Algorithm

It is known that moving average filter with narrow window has a smoothing effect on the signal and the moving average filter with wide window can get the general trend of a signal. That means we can reduce abrupt motion artifacts noise and get the baseline signal in the actual PPG signal through moving average filtering. Now some previous works present that moving average filter is very useful to remove high-frequency noise and intermittent motion artifact. It can reduce effects of mutations on the PPG signal waveform [13]. However, it is difficult to remove a large amplitude motion artifact, and the higher the filter order, the worse the quality of the waveform [14]. We take advantage of the most simple moving average filter:

$$y[n] = \frac{1}{N}\sum_{i=0}^{N-1}(x[n-i]), n = N, N+1, \ldots, L \tag{5}$$

Where N is the widow size and L is the data length. We design two filters to reduce noises in the original signal utilizing the different characteristics of moving average filtering.

3.1 Baseline Wandering Removal

We take advantage of the low-pass characteristic of moving average filter to design the baseline wandering removal algorithm. As the frequency of baseline wandering is far lower than heart beats, we can use moving average filter to get the baseline wandering signal and then reduce it from the original signal. The window size is set to be:

$$N_{BW\_} = \frac{N_S \cdot 60}{BPM} \tag{6}$$

In formula (7), N_S is the number of sampling points per second. The output signal with base wandering removal $\boldsymbol{S_{BW\_}}$ is acquired as following steps:

Step 1. Get a temperate baseline wandering signal $\boldsymbol{BW_{tmp}}$ from the original signal $\boldsymbol{S}$ using moving average filter ($\boldsymbol{MAF}$) with window size $N_{BW\_}$:

$$\boldsymbol{BW_{tmp}} = \boldsymbol{MAF}(\boldsymbol{S}, N_{BW\_}) \tag{7}$$

Step 2. To compensate for the lost data and get the complete baseline wandering signal $\boldsymbol{BW}$:

$$\begin{cases} BW[1:P] = \boldsymbol{BW_{tmp}}[1:P] + \boldsymbol{BW_{tmp}}[1] - \boldsymbol{BW_{tmp}}[P+1] \\ BW[P+1:Q] = \boldsymbol{BW_{tmp}} \\ BW[Q+1:L] = \boldsymbol{BW_{tmp}}[Q - N_{BW\_}:Q-P] + \boldsymbol{BW_{tmp}}[Q-P] \\ \quad -\boldsymbol{BW_{tmp}}[Q - N_{BW\_} - 1] \end{cases} \tag{8}$$

where $P = \begin{cases} \frac{N_{BW\_}-1}{2}, N_{BW\_} is\ odd \\ \frac{N_{BW\_}}{2}, N_{BW\_} is\ even \end{cases}$, and $Q = L - N_{BW\_} + P + 1$.

Step 3. Subtract the baseline wandering signal from the original signal:

$$\boldsymbol{S_{BW\_}} = \boldsymbol{S} - \boldsymbol{BW} \tag{9}$$

3.2 Motion Artifact Removal

After removal of baseline wandering, we need to remove the motion artifacts. As moving average filter has a perfect inhibition of the signal near the cut-off frequency, we can reduce rhythmic motion artifacts by moving average filter with window size $N_{MA\_}$. $N_{MA\_}$ is the cycle of motion artifacts in discrete domain. If the motion artifact is irregular, then $N_{MA\_}$ can be set as a constant to smooth the signal. The motion artifact removal algorithm is described specifically as following:

Step 1. From the normalized auto correlation function (NACF) [15] of accelerometer signal, determine whether there is rhythmic motion artifact or not. If the peak value of NACF is larger than the setting threshold, the rhythmic motion artifact exits and set the peak point as $N_{MA\_}$. If the peak value is lower than the setting threshold, $N_{MA\_}$ is set to be a constant.

Step 2. Get a temperate signal $\boldsymbol{Y_{tmp}}$ without motion artifacts using $\boldsymbol{MAF}$ with window size of $N_{MA\_}$:

$$\boldsymbol{Y_{tmp}} = \boldsymbol{MAF}(\boldsymbol{S_{BW\_}}, N_{MA\_}) \tag{10}$$

Step 3. Estimate the period T of $\boldsymbol{Y_{tmp}}$ in the discrete domain by average magnitude difference function (AMDF) [16]. And the result of BPM detection is $BPM = N_s \cdot 60/T$.

Step 4. To compensate for the lost data and get the complete signal with amplitude suppressed $\boldsymbol{Y}$.

$$\begin{cases} Y[1:\mu] = \boldsymbol{Y_{tmp}}[T-\mu : T-1] \\ Y[\mu+1:\tau] = \boldsymbol{Y_{tmp}} \\ Y[\tau+1:L] = \boldsymbol{Y_{tmp}}[\tau-\mu-T+2 : L-\mu-T+1] \end{cases} \tag{11}$$

Where $\mu = \begin{cases} \frac{N_{MA\_}-1}{2}, N_{MA\_} is\ odd \\ \frac{N_{MA\_}}{2}, N_{MA\_} is\ even \end{cases}$, $\tau = L - N_{MA\_} + \mu + 1$.

Step 5. To compensate for the amplitude attenuation and get the reconstructed signal $\boldsymbol{S_R}$:

$$\boldsymbol{S_R} = \boldsymbol{Y}/A(x) \tag{12}$$

Where $A(x) = x^3 - 2x^2 + 1, x = \frac{N_{MA\_}}{T}$. $A(x)$ is acquired by curve fitting from the amplitude-frequency curve of moving average filter.

3.3 Dynamic Monitoring

Because of continuous changes of motion state and heartbeat in the long-time monitoring, the coefficients of moving average filters need to be changed relatively in order to remove motion artifacts more effectively and improve the accuracy of BPM detection. The flow chart of the whole algorithm is shown as Fig. 3 where $MAF_{BW\_}$ is the baseline wandering removal algorithm and $MAF_{MA\_}$ is the motion artifact removal algorithm. We call this method as batch processing method. We select 3–4 s data as a batch and set $N_{BW\_}$ in the next batch to be T in the current batch (except initialization in the first batch). We assume heart beats cannot change suddenly in 3–4 s.

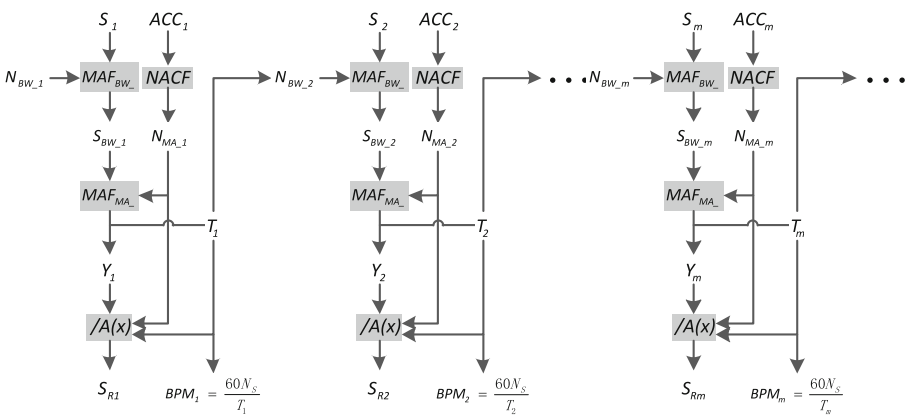

Fig. 3. Batch processing method of dynamic monitoring.

4 Results

Firstly, we collect the photoelectric signal and accelerometer signal in different rhythmic motion states those will affect in-ear PPG signal to improve the artifacts existence criterion. Figure 4 simply shows the data under 6 common condition in daily life. The tester wears the heart rate detecting earphone and makes the corresponding action according to the instruction in order. The earphone can transport data out by bluetooth connecting. As long as there is rhythmic motion artifact in the PPG signal, the accelerometer signal has the similar rhythm. Conversely, we cannot determine whether the rhythmic motion artifact exits or not when the accelerometer has a rhythmic. So in the Step.1 of motion artifact removal algorithm, the sum amplitude of 3-axis accelerometer should be taken into consideration. We set two thresholds when we estimate the coefficient $N_{MA}\_$. $N_{MA}\_$ is set to be the period of accelerometer signal only when the sum amplitude of all three axis is larger than the first threshold and the peak value of NACF is larger than the second threshold. During continuous monitoring, when the point of NACF is less than the previous T, $N_{MA}\_$ is set to be the period of accelerometer signal. In other cases, $N_{MA}\_$ is set to be a constant. Table 1 shows the accelerometer data analysis under the 6 common states. After a lot of experiments, in this paper our first threshold is 3 g, the second is 0.5 and the constant is 7 (about 9 Hz).

Secondly, we select the worst signal acquired in the high leg lifting case to verify the effectiveness of base wandering removal algorithm $MAF_{BW}\_$ and motion artifact removal algorithm $MAF_{MA}\_$. As shown in Fig. 5, we intercept 500 points of the data acquired during rapid leg lifting. In Fig. 5(b), $N_{BW}\_$ is assigned to be 63 as sampling rate is 62.5 Hz and heart rate is commonly 1 Hz. We calculate the amplitude of the baseline BW. BW is reduced from 439.92 to 23.83. As the sum amplitude of 3-axis accelerometer signal is larger than 3 g and from the NACF of y-axis accelerometer signal as shown in Fig. 6(a) we set $N_{MA}\_$ to be 11. Then from the AMDF of the

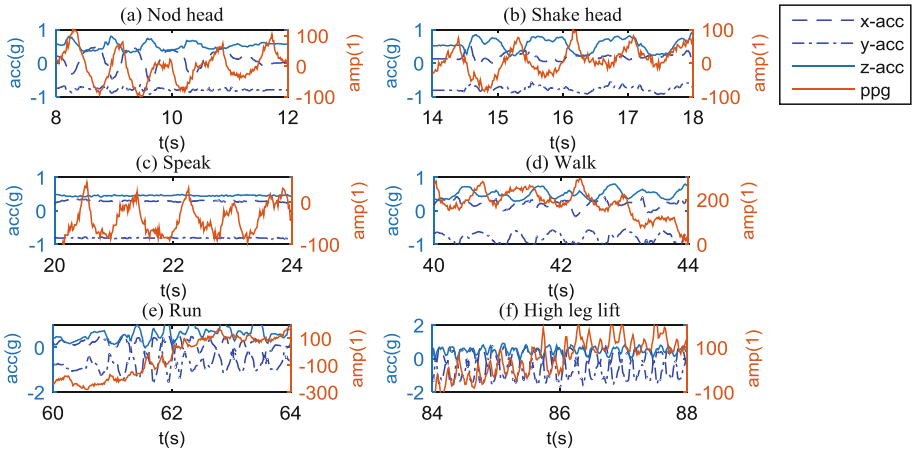

Fig. 4. Signals in 6 common cases.

Table 1. Accelerometer data analysis in 6 common cases.

Cases	AMP ACC/g			SUM of ACC/g	NACF of MAX[X,Y,Z]	
	X	Y	Z		Point	Value
Nod	1.0469	0.2969	0.4844	1.8282	44	0.5793
Shake	0.6094	0.3906	0.7813	1.7813	67	0.5632
Speak	0.1875	0.0781	0.0938	0.3594	92	0.1581
Walk	0.6875	0.7031	0.5938	1.9844	36	0.6513
Run	*1.1719*	*1.8281*	*1.4688*	*4.4688*	*17*	*0.5291*
High Leg lift	*1.5781*	*2.1875*	*1.1563*	*4.9219*	*11*	*0.6298*

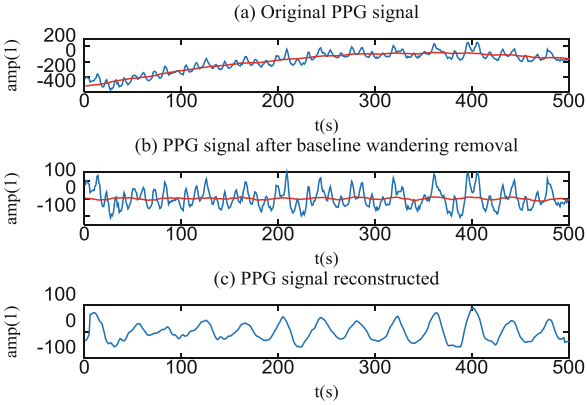

Fig. 5. Result of baseline wandering removal and motion artifact removal.

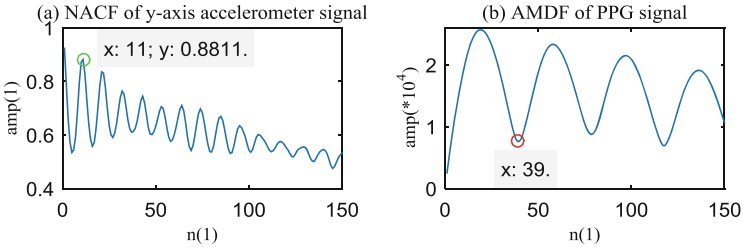

Fig. 6. NACF and AMDF in Fig. 5(c).

temperate reconstructed signal as shown in Fig. 6(b), T is set to be 39 and the result of BPM detection is 96. Then the amplitude compensation coefficient is 0.8633. The reconstructed signal is finally showed as Fig. 5(c). Obviously, the morphology of reconstructed signal is more clear than the original signal and we can exact BPM from it accurately.

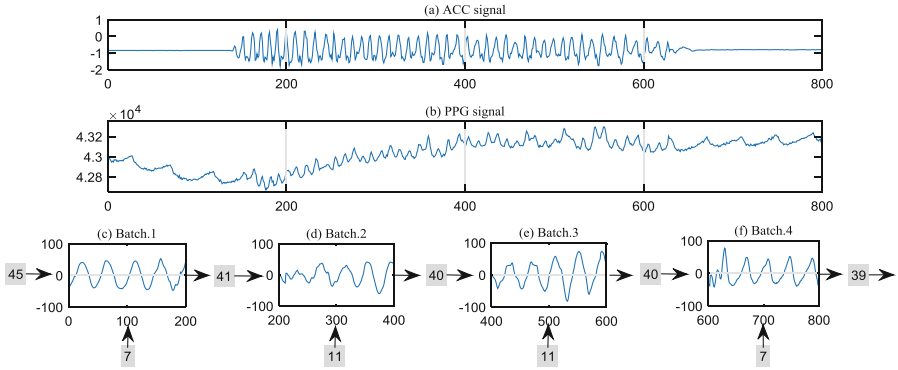

Fig. 7. Result of dynamic monitoring.

Thirdly, we select 200 points data as a batch and the batch processing result is shown in Fig. 7, where x label is discrete sequence, y label is amplitude. The right arrow represents $N_{BW\_}$ from the current batch to the next. The up arrow represents $N_{MA\_}$ determined from the current accelerometer signal. However, the motion artifacts cannot exactly start at the beginning of one batch and finish at the end of one batch, so in Fig. 7(d) and (f) there are a little distortion in the signals. The distortion will not affect the accuracy of BPM estimation.

Finally, we make a comparative experiment between the proposed algorithm and adaptive filtering referenced with a medical instrument VS800, which is a vital sign monitoring product of Mindray company. We record the time and BPM on the display screen of VS800 by video. Tester wears our device with his finger clipped by the VS800's probe and does some daily life actions during 10 min. We collect our device's data to a computer whose time is synchronized with the VS800 and process the signal by different algorithms simutaneously. NLMS is shown as formula (13):

$$\begin{cases} y = H \cdot \omega^T \\ e = x - y \\ H = H + \frac{\alpha}{\beta + \omega \cdot \omega^T} \cdot e \cdot \omega \end{cases} \tag{13}$$

RLS recursion equations can is obtained as formula (14):

$$\begin{cases} g = \left(\frac{P \cdot \omega^T}{\delta + \omega \cdot P \cdot \omega^T}\right)^T \\ y = H \cdot \omega^T \\ e = x - y \\ H = H + g \cdot e \\ P = \frac{1}{\delta}(P - g \cdot \omega^T \cdot P) \end{cases} \tag{14}$$

The result of the BPM detected is shown in Fig. 8 whose y label is detecting BPM and x label is reference BPM. The red crosses are out of the interval ±5 bpm and blue cycles are in the interval. The detecting accuracy of the proposed method is the highest and 7%–10% higher than adaptive filtering. The statistical analysis of the result is

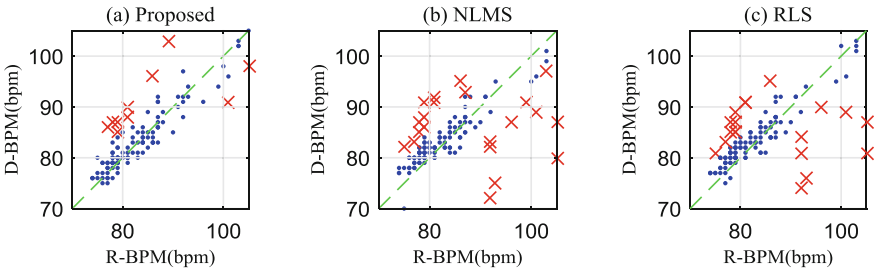

Fig. 8. Comparative experiment with a reference signal (Color figure online)

Table 2. Statistical analysis of the result in Fig. 8.

Algorithm	Accuracy/%	MSE	SROCC	PROCC	PLCC
Proposed	*91.67*	*5.2091*	*0.8659*	*0.7318*	*0.8851*
NLMS	80.83	6.3608	0.7103	0.5918	0.6368
RLS	84.17	5.6436	0.7253	0.6066	0.7085

shown in Table 2. SROCC is spearman rank order correlation coefficient. KROCC is kendall rank order correlation coefficient. PLCC is pearson linear correlation coefficient. The statistical result indicates that the BPM detected by the proposed algorithm is more accurate and has a stronger correlation to the reference BPM.

5 Conclusion

In this paper, with additional accelerometer, we propose algorithms based on moving average filtering which effectively remove noises of base wandering and motion artifacts in ear PPG signal. During continuous monitoring, the coefficients of filters adaptively change through a batch processing method. We can reconstruct better waveform from the corrupted original signal and improve the accuracy of BPM detection.

References

1. Tamura, T., et al.: Wearable photoplethysmographic sensors—past and present. Electronics **3**(2), 282–302 (2014)
2. Millasseau, S.C., et al.: Contour analysis of the photoplethysmographic pulse measured at the finger. J. Hypertens. **24**(8), 1449–1456 (2006)
3. Lee, Y., et al.: Development of a wristwatch-type PPG array sensor module. In: 2011 IEEE International Conference on Consumer Electronics-Berlin (ICCE-Berlin) (2011)
4. Budidha, K., Kyriacou, P.A.: The human ear canal: investigation of its suitability for monitoring photoplethysmographs and arterial oxygen saturation. Physiol. Meas. **35**(2), 111–128 (2014)

5. Ming-Zher, P., Swenson, N.C., Picard, R.W.: Motion-tolerant magnetic earring sensor and wireless earpiece for wearable photoplethysmography. IEEE Trans. Inf. Technol. Biomed. **14**(3), 786–794 (2010). A Publication of the IEEE Engineering in Medicine & Biology Society
6. Sweeney, K.T., et al.: Artifact removal in physiological signals-practices and possibilities. IEEE Trans. Inf Technol. Biomed. **16**(3), 488–500 (2012). A Publication of the IEEE Engineering in Medicine & Biology Society
7. Han, H., Kim, J.: Artifacts in wearable photoplethysmographs during daily life motions and their reduction with least mean square based active noise cancellation method. Comput. Biol. Med. **42**(4), 387–393 (2011)
8. Gibbs, P.T., Wood, L.B., Asada, H.H.: Active motion artifact cancellation for wearable health monitoring sensors using collocated MEMS accelerometers. In: Proceedings of SPIE - The International Society for Optical Engineering, vol. 5765, pp. 811–819 (2005)
9. Lee, B., et al.: Improved elimination of motion artifacts from a photoplethysmographic signal using a Kalman smoother with simultaneous accelerometry. Physiol. Meas. **31**(12), 1585–1603 (2010)
10. Shi Ping, Y.H.: Principles of photoplethysmography and its applications in physiological measurements. J. Biomed. Eng. **30**(4), 899–904 (2013)
11. Allen, J.: Photoplethysmography and its application in clinical physiological measurement. Physiol. Meas. **28**(3), R1–39 (2007)
12. Zhang, Z.: Photoplethysmography-based heart rate monitoring in physical activities via joint sparse spectrum reconstruction. IEEE Trans. Biomed. Eng. **62**(8), 1902–1910 (2015)
13. Lee, J.: Motion artifacts reduction from PPG using cyclic moving average filter. Technol. Health Care Official J. Eur. Soc. Eng. Med. **22**(3), 409–417 (2014)
14. Lee, H.W., et al.: The periodic moving average filter for removing motion artifacts from PPG signals. Int. J. Control Autom. Syst. **5**(6), 701–706 (2007)
15. Yousefi, R., Nourani, M., Panahi, I.: Adaptive cancellation of motion artifact in wearable biosensors. In: Conference: International Conference of the IEEE Engineering in Medicine & Biology Society IEEE Engineering in Medicine & Biology Society Conference (2012)
16. Hui, L., Dai, B.Q., Wei, L.: A pitch detection algorithm based on AMDF and ACF. In: IEEE International Conference on Acoustics (2006)